MICROPLANE MODEL FOR CYCLIC TRIAXIAL BEHAVIOR OF CONCRETE

By Joško Ožbolt[1] and Zdeněk P. Bažant,[2] Fellow, ASCE

ABSTRACT: A recently proposed microplane model, which describes not only cracking but also general nonlinear triaxial response, is extended to cyclic loading and the rate effect, and is implemented in a three-dimensional finite element code. The material properties are characterized separately on planes of various orientations within the material, called the microplanes, on which no tensorial invariance requirements need to be observed. The state of each microplane is described by normal deviatoric and volumetric strains, and by shear strain. To avoid spurious localization instabilities due to strain softening and the consequent mesh-sensitivity problems, the concept of nonlocal continuum with local strain is adopted. The rate effect is introduced by combining the damage model on each microplane with the Maxwell rheologic model. The results of finite element analysis of some basic cases on the material level, as well as of plain concrete specimens loaded in bending and compression, are demonstrated. The calculated responses yield hysteretic loops of an approximately correct area and correct initial unloading slope. For shear, the calculated loops exhibit the well-known pinched form.

INTRODUCTION

The microplane model, formulated for concrete in Bažant (1984) and Bažant and Oh (1985), represents a constitutive model in which the material is characterized by a relation between the stress and strain components on planes of various orientations, which may be imagined to represent the damage planes or weak planes in the microstructure, such as the contact layers between aggregate pieces in concrete. The history of the general approach underlying the microplane model (Taylor 1938; Batdorf and Budianski 1949; Zienkiewicz and Pande 1977) has been given in detail earlier [e.g., Bažant and Oh (1985) and Bažant and Prat (1988)]. The latest version of the microplane model, developed by Bažant and Prat (1988), was shown capable of predicting the behavior of concrete in monotonic loading for a broad range of stress and strain conditions using only a few material parameters.

The nonlocal continuum concept (Eringen 1965, 1966; Kröner 1968; Krumhansl 1968; Eringen and Edelen 1972) whose adaptation in the form of nonlocal damage (Pijaudier-Cabot and Bažant 1987; Bažant and Pijaudier-Cabot 1988) has proven to provide an effective localization limiter, prevent spurious mesh sensitivity, and allow correct modeling of the size effect (Bažant and Lin 1988), has been combined with the microplane model in Bažant and Ožbolt (1990b). This provided a general material model capable of representing both nonlinear triaxial behavior and fracture. In conjunction with the nonlocal concept, this model was implemented in a finite element code. Its capabilities of realistically predicting the structural response were demonstrated in a number of numerical examples.

In the present work [based on a recent work by Bažant and Ožbolt (1990a)], the microplane model from Bažant and Prat (1988) is improved and is also extended to cyclic loading, as well as to the rate effect, which is important for cyclic loading. A kinematic constraint is used, i.e., the total strain vector on each microplane is assumed to be the resolved component of the macroscopic strain tensor. The microplane strains are split into volumetric, deviatoric, and shear components. The shear strain vector is further split into two orthogonal components. For each microplane strain component at each integration point of each finite element, the main characteristics of the load history are stored during the calculations. The numerical integration of the time step is based on the previously proposed exponential algorithm. The new model is implemented in a three-dimensional finite element code. [A similar but in some respects different version of a microplane model for cyclic loading is being developed in a parallel project by Hasegawa and Bažant (1991).]

To demonstrate the capability of the present generalization of the microplane model in simulating the cyclic and rate effects in plain concrete, the results of several numerical studies are presented, including: cycling in tension, cycling in compression, and cycling in shear, all calculated only for a small material element. Moreover, cyclic finite element analysis including the rate effect is performed for the cases of the three-point bending of a beam and the uniaxial compression test. The results of these numerical analyses are compared with test results.

REVIEW OF MICROPLANE MODEL

Basic Hypotheses and Strain Components

Hypothesis 1

Each microplane resists both the normal and shear strains, which are assumed to represent the resolved components of the macroscopic strain tensor ε_{ij}.

This hypothesis represents a kinematic constraint and yields the relations [see Bažant and Prat (1988)]:

$$\boldsymbol{\varepsilon}_i = n_i \varepsilon_{ij} \quad \ldots\ldots (1a)$$

$$\varepsilon_N = n_i n_j \varepsilon_{ij} \quad \ldots\ldots (1b)$$

$$\varepsilon_D = n_i n_j \varepsilon_{ij} - \varepsilon_V \quad \ldots\ldots (1c)$$

$$\boldsymbol{\varepsilon}_T = \varepsilon_M \mathbf{m} + \varepsilon_k \mathbf{k} \quad \ldots\ldots (2a)$$

$$\varepsilon_M = \mathbf{m}\boldsymbol{\varepsilon}_T = m_i n_j \varepsilon_{ij} \quad \ldots\ldots (2b)$$

$$\varepsilon_K = \mathbf{k}\boldsymbol{\varepsilon}_T = k_i n_j \varepsilon_{ij} \quad \ldots\ldots (2c)$$

where latin lowercase subscripts refer to Cartesian coordinates x_i (i = 1, 2, 3); $\boldsymbol{\varepsilon}$ = the strain vector on a microplane whose unit normal is n_i; ε = magnitude of $\boldsymbol{\varepsilon}$; $\boldsymbol{\varepsilon}_T$ = the tangential vector component of $\boldsymbol{\varepsilon}$; $\mathbf{m}$ and $\mathbf{k}$ = unit coordinate vectors defined in advance for each microplane [Fig. 1(*a*)]; ε_M and ε_K = in-plane components of vector $\boldsymbol{\varepsilon}_T$ in the direction of vectors $\mathbf{m}$ and $\mathbf{k}$; and $\boldsymbol{\varepsilon}_N$ = the vector of the normal strain component of $\boldsymbol{\varepsilon}$ on the microplane [Fig. 1(*a*)]. The normal strain vector is separated into volumetric

[1]Res. Engr., Institut für Werkstoffe im Bauwesen, Universität Stuttgart, Germany; formerly, Visiting Scholar, Dept. of Civ. Engrg., Northwestern University, Evanston, IL 60208.

[2]Walter P. Murphy Prof. of Civ. Engrg., Northwestern Univ., Evanston, IL.

Note. Discussion open until December 1, 1992. To extend the closing date one month, a written request must be filed with the ASCE Manager of Journals. The manuscript for this paper was submitted for review and possible publication on May 23, 1991. This paper is part of the ***Journal of Engineering Mechanics***, Vol. 118, No. 7, July, 1992. ©ASCE, ISSN 0733-9399/92/0007-1365/$1.00 + $.15 per page. Paper No. 1934.

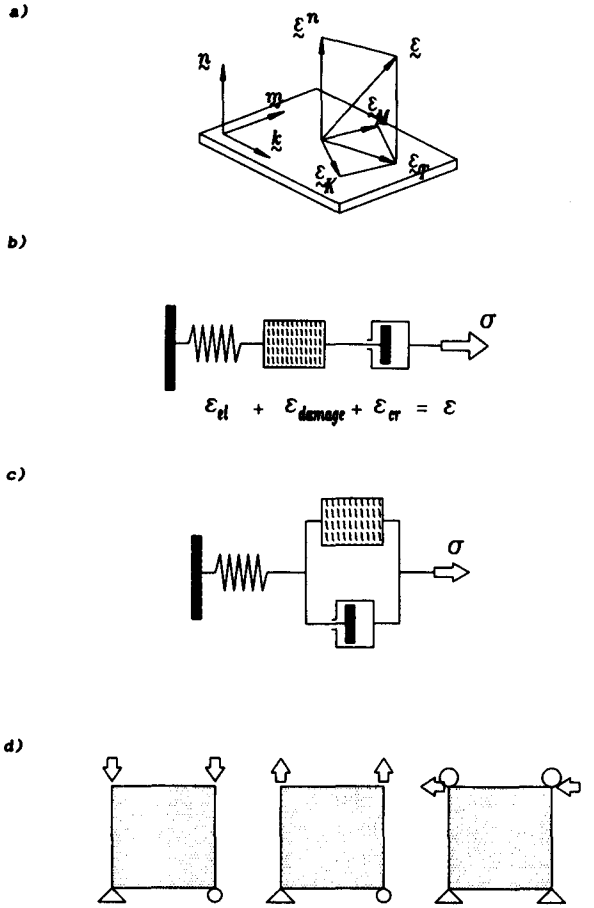

FIG. 1, (a) Stress and Strain Components on Each Microplane; (b) Maxwell Rheological Model with Damage for Each Microplane Strain Component; (c) Kelvin Type of Rheological Model; (d) Loading Cases Analyzed

strain $\varepsilon_V = \varepsilon_{kk}/3$ and deviatoric strain $\varepsilon_D = \varepsilon_N - \varepsilon_V$. In contrast to the originally proposed model (Bažant and Prat 1988), the in-plane shear strain vector $\boldsymbol{\varepsilon}_T$ is split into two in-plane components (ε_M and ε_K). In Bažant and Prat's original version of the general microplane model, the shear component $\boldsymbol{\varepsilon}_T$ has been characterized by its magnitude ε_T (which is always nonnegative) and the corresponding tangential stress vector $\boldsymbol{\sigma}_T$ has been considered to be always parallel to $\boldsymbol{\varepsilon}_T$. That simplifying assumption, which is the simplest possible, seems adequate for the monotonic loading or nearly monotonic loading, and in a crude manner perhaps also for the first unloading. But it is obviously inadequate for cyclic loading, one reason being that always $\varepsilon_T \geq 0$ according to that assumption, and another that $\boldsymbol{\sigma}_T$ and $\boldsymbol{\varepsilon}_T$ can obviously become nonparallel. The choice of coordinate vector $\mathbf{m}$ within the microplane is arbitrary (although, once chosen, vector $\mathbf{m}$ must be kept fixed). The other coordinate vector $\mathbf{k}$ is then obtained as $\mathbf{k} = \mathbf{m} \times \mathbf{n}$ [Fig. 1(*a*)]. To minimize directional bias, the directions of microplane

shear strain components are chosen as follows: for the first microplane, $\mathbf{m} \perp \mathbf{z}$, $m_3 = 0$; for the second, $\mathbf{m} \perp \mathbf{x}$, $m_1 = 0$; for the third, $\mathbf{m} \perp \mathbf{y}$; $m_2 = 0$, etc. This achieves that various $\mathbf{m}$-directions are represented nearly evenly, as required by coordinate frame indifference. (Better, one could generate the directions of $\mathbf{m}$ within each microplane randomly.)

Hypothesis 2

The response on each microplane is assumed to depend on the mean lateral strain ε_L, which is approximately equivalent to assuming that it depends on the volumetric strain $\varepsilon_V = \varepsilon_{kk}/3$ (aside from ε_N and ε_D). (This feature was found to be necessary for modeling triaxial test data for very high confining pressures, but not other data.)

Hypothesis 3

The stress-strain curves of each microplane are assumed to be path-independent as long as there is no unloading on this microplane. During unloading and reloading, which is defined separately on each microplane, the curve of stress difference versus strain difference from the state at the start of unloading or reloading is also assumed to be path-independent.

Thus, all the macroscopic path-dependence is produced by various combinations of loading and unloading on various microplanes. It may be noted that some microplanes may get unloaded even for macroscopically monotonic or virgin loading, thus making the response path-dependent. The number of possible macroscopic path directions is enormous (for 21 microplanes there are 2^{21} possible tantential stiffness matrices in each loading step, due to all possible combinations of loading and unloading).

Hypothesis 4

The volumetric and deviatoric responses on each microplane are assumed to be mutually independent. (This, of course, greatly simplifies data fitting and was shown to suffice to fit each test data set considered.) However, shear components are assumed to be dependent on volumetric strain in the case of volumetric compression. This was introduced since otherwise the response of concrete in the case of compression with high lateral confinement would not be possible to predict.

Microplane Stress-Strain Relations

In the case of virgin loading, the behavior for each microplane strain component is described, according to the foregoing hypotheses, by path-independent total stress-strain relations of the form:

$$\sigma_V = F_V(\varepsilon_V) \quad \ldots\ldots (3a)$$

$$\sigma_D = F_D(\varepsilon_D) \quad \ldots\ldots (3b)$$

$$\sigma_M = F_M(\varepsilon_M) \quad \ldots\ldots (3c)$$

$$\sigma_K = F_K(\varepsilon_K) \quad \ldots\ldots (3d)$$

For two reasons, namely representation of unloading and application of the nonlocal damage concept, it is convenient to cast the total stress-strain relations in the form of continuum damage mechanics:

$$\sigma_V = C_V \varepsilon_V \quad \ldots\ldots (4a)$$

$$\sigma_D = C_D\varepsilon_D \quad \ldots\ldots (4b)$$

$$\sigma_M = C_M\varepsilon_M \quad \ldots\ldots (4c)$$

$$\sigma_K = C_K\varepsilon_K \quad \ldots\ldots (4d)$$

in which, except for volumetric compression

$$C_V = C_V^0(1 - \omega_V) \quad \ldots\ldots (5a)$$

$$C_D = C_D^0(1 - \omega_D) \quad \ldots\ldots (5b)$$

$$C_M = C_M^0(1 - \omega_M) \quad \ldots\ldots (5c)$$

$$C_K = C_K^0(1 - \omega_K) \quad \ldots\ldots (5d)$$

where C_V, C_D, C_M, and C_K represent the secant moduli; $C_V = F_V(\varepsilon_V)/\varepsilon_V$, $C_D = F_D(\varepsilon_D)/\varepsilon_D$, $C_M = F_M(\varepsilon_M)/\varepsilon_M$, $C_K = F_K(\varepsilon_K)/\varepsilon_K$; and C_V^0, C_D^0, C_M^0, C_K^0 are the initial values of C_V, C_D, C_M, and C_K; and ω_V, ω_D, ω_M, and ω_K are the volumetric damage, deviatoric damage, and shear damage on the microplane level. The secant shear moduli C_M and C_K must be defined by the same functions of the corresponding shear strain components. The inital shear moduli for both shear components are equal for both directions, $C_M^0 = C_K^0$. Best fits of selected typical test data for concrete have been obtained using the following approximation for virgin loading:

$$\text{for } \varepsilon_V \geq 0: \quad \omega_V = 1 - \exp\left[-\left(\frac{\varepsilon_V}{e_1}\right)^m\right] \quad \ldots\ldots (6)$$

$$\text{for } \varepsilon_D \geq 0: \quad \omega_D = 1 - \exp\left(-\left|\frac{\varepsilon_D}{e_1}\right|^m\right) \quad \ldots\ldots (7a)$$

$$\text{for } \varepsilon_D < 0: \quad \omega_D = 1 - \exp\left(-\left|\frac{\varepsilon_D}{e_2}\right|^n\right) \quad \ldots\ldots (7b)$$

$$\omega_M = 1 - \exp\left(-\left|\frac{\varepsilon_M}{e_5}\right|^k\right) \quad \ldots\ldots (8a)$$

$$\omega_K = 1 - \exp\left(-\left|\frac{\varepsilon_K}{e_5}\right|^k\right) \quad \ldots\ldots (8b)$$

in which $e_5 = e_3$ if $\varepsilon_V \geq 0$, and $e_5 = e_3 - e_4\varepsilon_V < 0$, where e_1, e_2, e_3, e_4, e_5, m, n, and k are empirical material constants. The dependence of e_5 on the volumetric strain ε_V reflects internal friction and represents an additional kinematic constraint of scalar type.

In the volumetric behavior, there is no damage ($\omega_V = 0$) and the response for virgin loading is described by:

$$\text{for } \varepsilon_V < 0: \quad C_V = C_V^0\left[\left(1 + \left|\frac{\varepsilon_V}{a}\right|\right)^{-p} + \left|\frac{\varepsilon_V}{b}\right|^q\right] \quad \ldots\ldots (9)$$

where a, b, p, and q are empirical constants.

Generalization to Unloading, Reloading, and Cyclic Loading

In the previous work (Bažant and Prat 1988), which was focused on monotonic loading, the rule for unloading was very simple, but it was possible to represent only the first unloading, and even that was with considerable errors compared to experiments. To model unloading, reloading, and cycling loading in general, and do so even for arbitrary triaxial stress states, more complex rules on the microplane level are needed. After much experimentation, the following unloading-reloading rules, which are different for each microplane strain component, have been chosen and verified.

In contrast to virgin loading, the stress-strain relations must be written in the incremental form:

$$d\sigma_V = C_V d\varepsilon_V \quad \ldots\ldots (10a)$$

$$d\sigma_D = C_D d\varepsilon_D \quad \ldots\ldots (10b)$$

$$d\sigma_M = C_M d\varepsilon_M \quad \ldots\ldots (10c)$$

$$d\sigma_K = C_K d\varepsilon_K \quad \ldots\ldots (10d)$$

where C_V, C_D, C_M, and C_K represent unloading-reloading tangent moduli. They are defined for each microplane component as follows (See Fig. 2):

$$C = C^0\alpha + (1 - \alpha)\frac{\sigma}{\varepsilon - \varepsilon_1} \quad \ldots\ldots (11a)$$

$$\text{for } \varepsilon > \varepsilon_p\varepsilon_1 = \varepsilon_p - \frac{\sigma_p}{C^0} + \beta(\varepsilon - \varepsilon_p) \quad \ldots\ldots (11b)$$

$$\text{for } \varepsilon \leq \varepsilon_p; \quad (\varepsilon_1 = 0) \quad \ldots\ldots (11c)$$

where σ_p and ε_p denote the positive or negative peak stress and the corresponding strain for each microplane component, taking values σ_p^+, ε_p^+ and σ_p^-, ε_p^- for the positive and negative peaks; and α and β are empiricially chosen constants lying between 0 and 1. The unloading-reloading rules for tension (positive) and compression (negative), given separately for each microplane component, are defined graphically in Fig. 2. In contrast to the theory of plasticity, such simple rules suffice because we deal with mutually independent variables rather than tensors (as in plasticity or continuum damage mechanics). At each microplane, the rules for ε_V, ε_D, ε_M, ε_T are independent of each other and also of the rules for the other microplanes at the same material point.

The virgin loading for each microplane strain component ε occurs if

$$\varepsilon\Delta\varepsilon \geq 0 \text{ and } (\varepsilon - \varepsilon^{\max})(\varepsilon - \varepsilon^{\min}) \geq 0 \quad \ldots\ldots (12)$$

where $\varepsilon^{\max}$ and $\varepsilon^{\min}$ are the maximum and minimum values of ε that have occurred so far; otherwise unloading or reloading takes place.

The response curves shown later in the figure provide justification of the foregoing rules.

Incremental Macroscopic Stress-Strain Relations

Incremental loading analysis requires the total stress-strain relations [(3)] to be differentiated; $d\sigma_V = C_V d\varepsilon_V + \varepsilon_V dC_V$, $d\sigma_D = C_D d\varepsilon_D + \varepsilon_D dC_D$, $d\sigma_M = C_M d\varepsilon_M + \varepsilon_M dC_M$, and $d\sigma_K = C_K d\varepsilon_K + \varepsilon_K dC_K$. For iterative

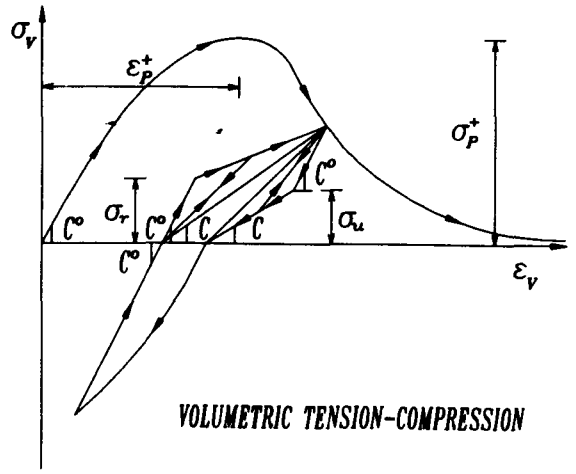

(a)

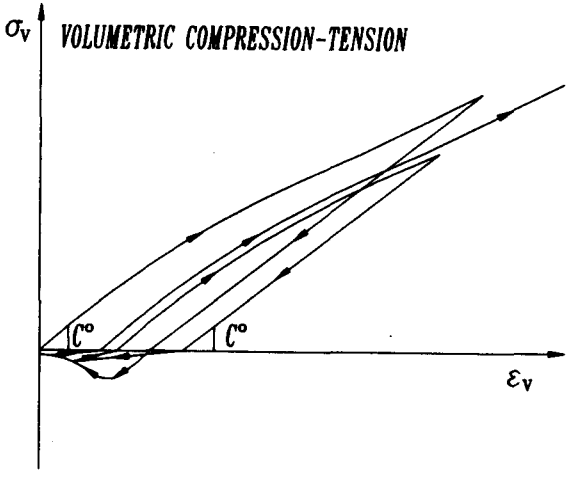

(b)

FIG. 2. Cyclic Rules for Microplane Strain Components: (a) Volumetric Tension-Compression; (b) Volumetric Compression-Tension

solution, it may be convenient to introduce incremental moduli $\hat{C}_V$, $\hat{C}_D$, $\hat{C}_M$, and $\hat{C}_K$, which may be equal or larger than C_V, C_D, C_M, and C_K. Then the incremental stress-strain relation has the form:

$$\Delta\sigma_V = \hat{C}_V\Delta\varepsilon_V - \Delta\sigma''_V \quad \ldots\ldots (13a)$$

$$\Delta\sigma_D = \hat{C}_D\Delta\varepsilon_D - \Delta\sigma''_D \quad \ldots\ldots (13b)$$

$$\Delta\sigma_M = \hat{C}_M\Delta\varepsilon_M - \Delta\sigma''_M \quad \ldots\ldots (13c)$$

$$\Delta\sigma_K = \hat{C}_K\Delta\varepsilon_K - \Delta\sigma''_K \quad \ldots\ldots (13d)$$

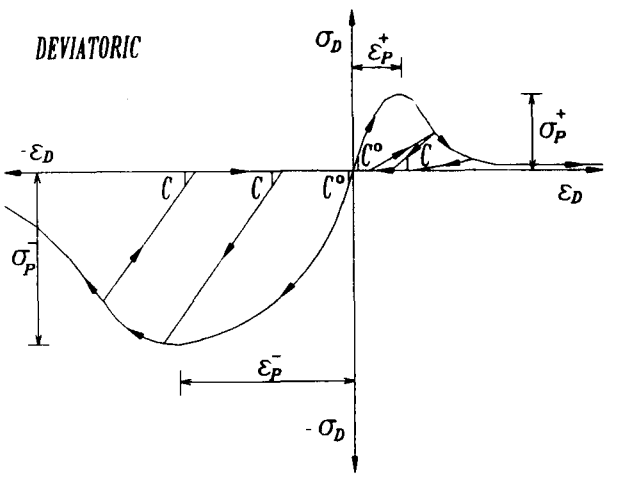

(c)

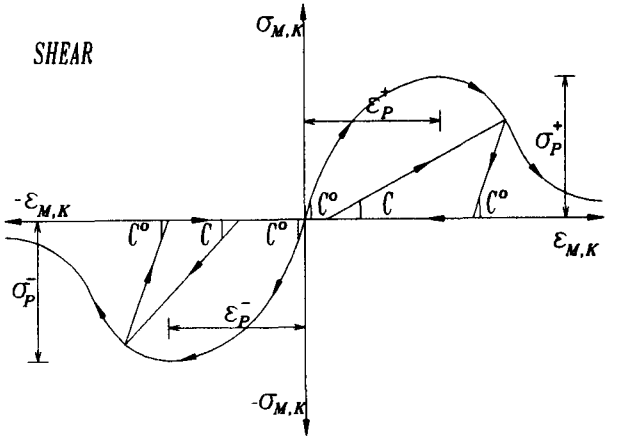

(d)

FIG. 2. Cyclic Rules for Microplane Strain Components: (c) Deviatoric; (d) Shear

in which

$$\Delta\sigma''_V = -\varepsilon_V\Delta C_V + (\hat{C}_V - C_V)\Delta\varepsilon_V \quad \ldots\ldots (14a)$$

$$\Delta\sigma''_D = -\varepsilon_D\Delta C_D + (\hat{C}_D - C_D)\Delta\varepsilon_D \quad \ldots\ldots (14b)$$

$$\Delta\sigma''_M = -\varepsilon_M\Delta C_M + (\hat{C}_M - C_M)\Delta\varepsilon_M \quad \ldots\ldots (14c)$$

$$\Delta\sigma''_K = -\varepsilon_K\Delta C_K + (\hat{C}_K - C_K)\Delta\varepsilon_K \quad \ldots\ldots (14d)$$

$\Delta\sigma''_V$, $\Delta\sigma''_D$, $\Delta\sigma''_M$, and $\Delta\sigma''_K$ are formally treated as inelastic stress increments in a step-by-step iterative solution.

The same as shown in previous work (Bažant and Ožbolt 1990), equilibrium of stresses between the micro- and macrolevels may be approximately enforced by the virtual work equation:

$$\frac{4\pi}{3}\Delta\sigma_{ij}\delta\varepsilon_{ij} = 2\int_S (\Delta\sigma_N\delta\varepsilon_N + \Delta\sigma_M\delta\varepsilon_M + \Delta\sigma_K\delta\varepsilon_K)F(\mathbf{n})\,dS \quad \ldots\ldots (15)$$

where $\mathbf{n}$ = the unit vectors normal to the microplanes; and $\delta\varepsilon_{ij}$, $\delta\varepsilon_N$, $\delta\varepsilon_M$, and $\delta\varepsilon_K$ = the small variations on the macro- and microlevels. The left-hand side of (15) represents the macroscopic work done in a unit sphere of the material, while the right-hand side represents the microscopic work done over the surface of the same sphere. The factor 2 is due to the fact that the integral needs to extend only over a hemisphere surface, S. $F(\mathbf{n})$ is a weight function of the normal directions $\mathbf{n}$ that can introduce anisotropy of the material in its initial state. For concrete we assume $F(\mathbf{n}) = 1$, which implies initial isotropy. Substituting (1), (2), (6)–(8), and (12), one can get from (15) the incremental macroscopic stress-strain relation:

$$\Delta\sigma_{ij} = C_{ijrs}\Delta\varepsilon_{rs} - \Delta\sigma''_{ij} \quad \ldots\ldots (16)$$

in which

$$C_{ijrs} = \frac{3\pi}{2}\int \left[n_in_jn_rn_sC_D + \frac{1}{3}n_in_j\delta_{km}(C_V - C_D) + \frac{1}{4}(m_im_j + m_jn_i) \right.$$

$$\left. \cdot (m_rn_s + m_sn_r)C_M + \frac{1}{4}(k_in_j + k_jn_i)(k_rn_s + k_sn_r)C_K \right] F(\mathbf{n})\,dS \quad \ldots. (17)$$

$$\Delta\sigma''_{ij} = \frac{3\pi}{2}\int_S \left[n_in_j(\Delta\sigma''_V + \Delta\sigma''_D) + \frac{1}{2}(m_in_j + m_jn_i)\,\Delta\sigma''_M \right.$$

$$\left. + \frac{1}{2}(k_in_r + k_jn_r)\,\Delta\sigma''_K \right] F(\mathbf{n})\,dS \quad \ldots\ldots (18)$$

C_{ijrs} = the macroscopic incremental material stiffness tensor, and $\Delta\sigma''_{ij}$ = the associated macroscopic inelastic stress increments.

Tensor C_{ijrs} can have different values depending on the choice of $\hat{C}_V$, $\hat{C}_D$, $\hat{C}_M$, and $\hat{C}_K$. There are three basic choices:

1. Setting $\hat{C}_V = C_V$, $\hat{C}_D = C_D$, $\hat{C}_M = C_M$, and $\hat{C}_K = C_K$ for all integration points, the resulting C_{ijrs} represent the secant stiffness tensor.
2. Setting $\hat{C}_V = C^0_V$, $\hat{C}_D = C^0_D$, $\hat{C}_M = C^0_M$, and $\hat{C}_K = C^0_K$, tensor C_{ijkm} must be equal to the isotropic tensor $C_{ijrs} = (K - 2G/3)\,\delta_{ij}\delta_{km} + G(\delta_{ik}\delta_{jm} + \delta_{im}\delta_{jk})$ where K, G = initial elastic bulk and shear moduli; and $K = E/3(1 - 2\nu)$ where E = Young's modulus and ν = Poisson's ratio.
3. With $\hat{C}_V = C'_V$, $\hat{C}_D = C'_D$, $\hat{C}_M = C'_M$, and $\hat{C}_K = C'_K$, where C'_V, C'_D, C'_M, and C'_K represent microplane tangent stiffness moduli, and C_{ijrs} represent the tangent stiffness tensor.

Computational efficiency is usually the highest for the second choice, for the following reasons: (1) Tensor C_{ijrs} is always the same, and so the structural stiffness matrix need not be to recalculated at each iteration of each loading step; (2) all the inelastic effects are represented by $\Delta\sigma''_{ij}$, a tensor of fewer components than C_{ijrs} (the iterative procedure in this case coincides with the well-known initial stiffness method); and (3) due to the fact that tensor C_{ijrs} is nonsymmetric, the use of the first or third approach would require a nonsymmetric equation system solver, which is rather demanding for computer time [it has been suggested that the use of a symmetric equation solver may be rendered possible by replacing in (16) $C_{ijrs}\Delta\varepsilon_{rs}$ with $\hat{C}_{ijrs}\Delta\varepsilon_{rs}$ where $\hat{C}_{ijrs} = (C_{ijrs} + C_{rsij})/2$ is the symmetric part of C_{ijrs}, and including the term $(C_{ijrs} - \hat{C}_{ijrs})\Delta\varepsilon_{rs}$ in the expression for the $\Delta\sigma''_{ij}$, but this usually leads to poor convergence].

The integrals in (15), (17), and (18) are evaluated numerically and the same integration scheme is used as described by Bažant and Ožbolt (1990b).

The material parameter values used in the calculations are the same as described by Bažant and Prat (1988), except parameter e_4, which is here a function of the volumetric strain rather than volumetric stress, and two additional constants α and β for each microplane component. Approximately optimal values of α and β have been obtained by fitting the set of cyclic test data. Computational experience using the present microplane model indicates that one may consider α and β to be constant for all concrete types.

Rate Effect

From experimental evidence it is well known that concrete stiffness, strength, and ductility are sensitive to the deformation rate. This is known as the rate effect. This effect is no doubt caused by creep in the bulk test specimen as well as time-dependent rupture of bonds in the fracture process zone, which both cause stress relaxation. The simplest model for relaxation is the Maxwell's spring dashpot model, which we adopt for each of the microplane strain components ε_V, ε_D, ε_M, and ε_K (Fig. 1*b*). Dropping for the moment the subscripts V, D, M, and K, the stress-strain relation for each microplane component may be written as

$$\dot{\sigma} + \frac{\sigma}{\rho} = C_t\dot{\varepsilon} \quad \ldots\ldots (19)$$

where ε = the total microplane strain including the flow strain (viscous or creep), the superimposed dots denote time derivatives, C_t = the tangent modulus for the microplane component, and ρ = a material parameter representing the relaxation time, whose value is assumed to be constant and the same for all microplane components (and of course for all microplane directions). Since the microplane stress-strain relations [(4)] are in a secant form, it is convenient to rewrite (19) also in the secant form:

$$\dot{\sigma} = C\dot{\varepsilon} - \frac{\sigma}{\lambda} \quad \ldots\ldots (20)$$

in which the following notations are introduced:

$$\frac{1}{\lambda} = \frac{1}{\rho} - \varepsilon\frac{\Delta C}{\Delta\varepsilon}\frac{\dot{\varepsilon}}{\sigma} \quad \ldots\ldots (21a)$$

$$C_t = \left(C + \varepsilon\frac{\Delta C}{\Delta\varepsilon}\right) \quad \ldots\ldots (21b)$$

$$\dot{\sigma} = \frac{\Delta\sigma}{\Delta t}, \qquad \dot{\varepsilon} = \frac{\Delta\varepsilon}{\Delta t} \qquad \text{(21c)}$$

Here λ = an apparent relaxation time and C = the secant modulus for the microplane strain component.

The present case of a simple Maxwell unit with a single relaxation time ρ is no doubt a simplification. We must expect that in reality the response is characterized by the Maxwell chain in which each unit has a different relaxation time and is described by an equation similar to (19). But such a more sophisticated model would be needed only if several orders of magnitude of the deformation rates were considered, which is not the case here.

Another possibility is to introduce a rheological model consisting of an elastic spring coupled in parallel with the damage and viscous units [Fig. 1(c)]. According to the current studies (Northwestern and Stuttgart universities) this model seems to be capable of predicting the behavior of the material over a very broad range of the loading rates. However, further work is needed in order to clarify whether this rheological model, coupled together with the microplane constitutive law, is really able to cover the broad range of loading rates.

Exponential Algorithm for Load or Time Step

Based on the kinematic constraint [(1)], the known macrostrains $\varepsilon_{ij(r)}$ and their known increments $\Delta\varepsilon_{ij(r)}$ can be used in every iteration of load or time step number r to calculate the strains and strain increments on each microplane. Then, the known values of $\varepsilon_N = \varepsilon_V + \varepsilon_D$, ε_M, ε_K, $\Delta\varepsilon_N = \Delta\varepsilon_V + \Delta\varepsilon_D$, $\Delta\varepsilon_M$, and $\Delta\varepsilon_K$, are used to calculate the stresses on each microplane by solving (13) or (20) with (21). Each of these equations could be solved by using a forward difference approximation or central difference approximation. However, such an approximation is often unstable when the stress-strain relation has a negative slope (strain softening), and, even if it remains stable, a large error is usually accumulated, with the result that the stress-strain curve obtained does not end at very large strain exactly at zero stress.

These drawbacks can be eliminated by the so-called exponential algorithm, initially developed for aging creep of concrete (Bažant 1971; Bažant and Wu 1974) and later extended to creep with strain softening (Bažant and Chern 1985; Bažant and Ožbolt 1990b). Here we extend the exponential algorithm to the microplane model with the rate effect. The basic principle that endows the exponential algorithm with high accuracy is that the integration formula is the exact solution of the differential equation [(20)] for the loading step under the assumption that the material properties, the loads, and the prescribed rates are constant in time.

For the rth time step, $\Delta t_r = t_{r+1} - t_r$, (20) can be rewritten in the form:

$$\dot{\sigma} + \frac{\sigma}{\lambda} = \bar{C}\dot{\varepsilon} \qquad \text{(22)}$$

where $\bar{C} = (C_r + C_{r+1})/2$ is considered to be constant during the step. λ is also considered to be constant during the step, and for best accuracy is evaluated from the average values of ε and σ in the step.

With constant λ and $\bar{C}$, we can integrate (22) exactly from time t_r to time t_{r+1}, using the same procedure as Bažant and Ožbolt (1990b) [(20)–(25)] did for the time-independent case. The exact solution of (20) is $\sigma(t) = Ae^{-\xi} + \bar{C}\lambda\dot{\varepsilon}$ where A = an integration constant and $\xi = (t - t_r)/\lambda$. From the

initial condition $\sigma = \sigma_r$ at $t = t_r$, it follows that $\sigma(t) = \sigma_r e^{-\xi} + (1 - e^{-\xi})\bar{C}\lambda\Delta\varepsilon$. For the end of the time step, $t = t_{r+1} = t_r + \Delta t$, we thus get

$$\sigma_{r+1} = \sigma_r + \Delta\sigma = \sigma_r e^{-\Delta z} + (1 - e^{-\Delta z})\bar{C}\frac{\Delta\varepsilon}{\Delta z} \qquad \text{(23)}$$

in which we denote $\Delta z = \Delta t/\lambda = \Delta t/\rho - \Delta C/\bar{C}$. Eq. (23) can be rewritten in the form of a pseudoelastic stress-strain relation on the level of each microplane stress component

$$\Delta\sigma = D\Delta\varepsilon - \Delta\sigma'' \qquad \text{(24)}$$

where

$$D = \frac{\bar{C}(1 - e^{-\Delta z})}{\Delta z} \qquad \text{(25a)}$$

$$\Delta\sigma'' = D\Delta\varepsilon'' \qquad \text{(25b)}$$

$$\Delta\varepsilon'' = (1 - e^{-\Delta z})\frac{\sigma_r}{D} \qquad \text{(25c)}$$

$D\Delta\varepsilon = \Delta\sigma_{el}$; and $\Delta\sigma_{el}$ and $\Delta\sigma''$ = the elastic and inelastic stress increments. Note that in the special case when there is no rate effect, $\rho \to \infty$, (24) is the same as for the time-independent microplane model (Bažant and Ožbolt 1990b). With subscripts V, D, M, and K attached, the foregoing formulas are used to determine the stress increments on each microplane, for both normal and tangential directions.

Note that in evaluating the secant moduli and damage [(3)–(11)], one must replace ε_r at time t_r with the instantaneous (i.e., time-independent) part of the total strain, i.e., with

$$\varepsilon_r^{\text{inst}} = \varepsilon_r - \sum_{s=1}^{r-1} \Delta\varepsilon_s^{\text{creep}} \qquad \text{(26)}$$

where $\Delta\varepsilon_s^{\text{creep}}$ = the time-dependent (viscous) parts of the microplane strain increments in the previous steps ($s = 1, 2, \ldots, r - 1$). Based directly on (19), one could here use $\Delta\varepsilon_s^{\text{creep}} \simeq (\sigma/\rho)\Delta t_s$ with σ and ρ taken as the average values in the step Δt_s. But it is more accurate to express $\Delta\varepsilon_s^{\text{creep}}$ according to the exponential algorithm modified by deleting the instantaneous part from (19)–(24). Thus, in analogy with (24)–(25)

$$\Delta\varepsilon_s^{\text{creep}} = (1 - e^{-\Delta\xi})\frac{\sigma_s}{D} \qquad \left(\Delta\xi = \frac{\Delta t}{\rho}\right) \qquad \text{(27)}$$

The values of the secant moduli and damage are then best calculated from (3)–(11) by replacing ε in the rth time step with $(\varepsilon_r^{\text{inst}} + \varepsilon_{r+1}^{\text{inst}})/2$.

The reason the foregoing algorithm is called exponential is that its formula characteristically involves an exponential function.

Another possible algorithm may be based on the total stress-strain relation [(4)]. In that case, the actual relaxation time ρ is used instead of λ in (21)–(24), and the inelastic stress increments then are $\Delta\sigma'' = (1 - e^{-\Delta\xi})\sigma_r + F(\varepsilon_{r+1}^{\text{inst}}) - (\varepsilon_{r+1}^{\text{inst}}/\varepsilon_r^{\text{inst}})F(\varepsilon_r^{\text{inst}})$ and $D = \bar{C}(1 - e^{-\Delta\xi})/\Delta\xi$.

On the macrolevel, the stress tensor increments are determined by numerical integration over the unit hemisphere (using 21-point numerical integration formula, in the present work), as already described.

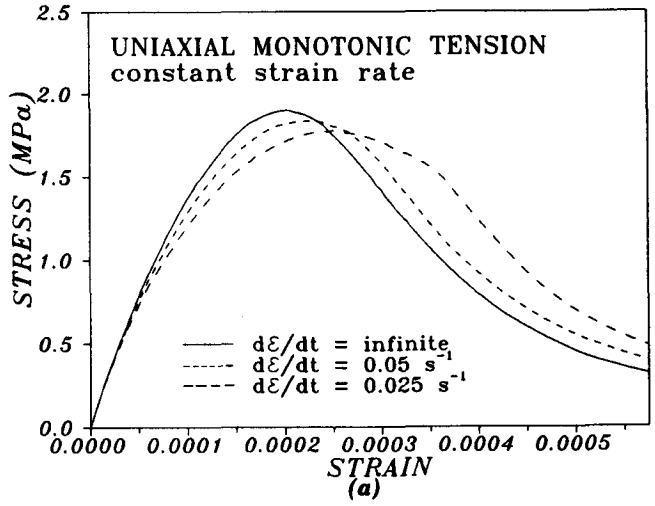

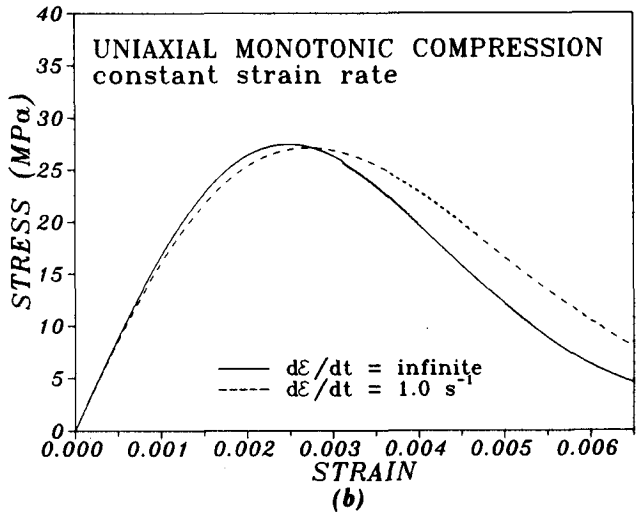

FIG. 3. Calculated Concrete Response under: (*a*) Monotonic Uniaxial Tension with Different Strain; (*b*) Monotonic Uniaxial Compression with Different Rates

Nonlocal Generalization of Microplane Model

In the classical, local continuum analysis by finite element method, strain localization leads to problems of instability, inobjectivity, and spurious mesh sensitivity (Bažant 1976; Bažant and Pijaudier-Cabot 1987). These problems can be circumvented by adopting the nonlocal continuum approach. An effective nonlocal concept is that recently proposed by Bažant and Pijaudier-Cabot (1987) in which only the variables associated with damage are nonlocal. This concept is implemented in the present cyclic microplane model. The method of implementation is basically the same as that already described

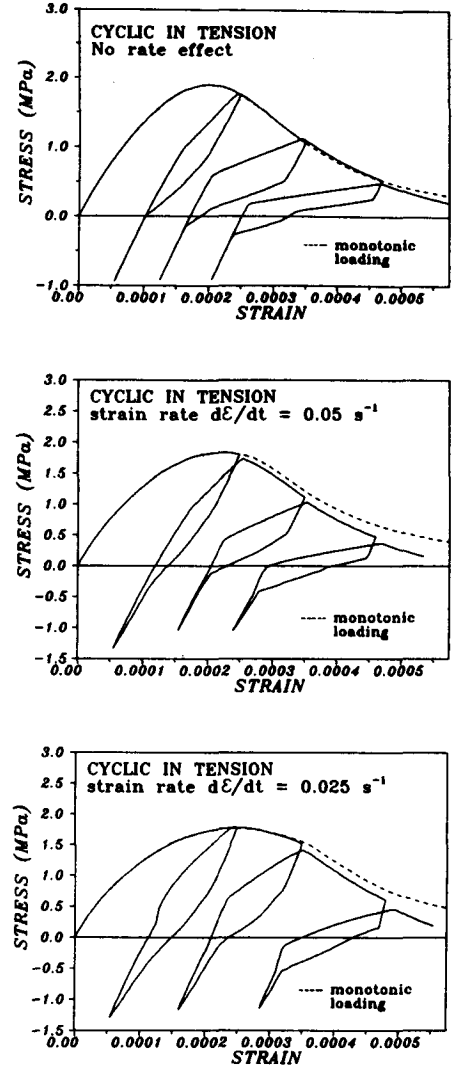

FIG. 4. Calculated Concrete Behavior in Uniaxial Cyclic Tension with Three Different Rates

by Bažant and Ožbolt (1990) for the case without rate effect. That paper also describes an effective numerical iterative algorithm for the loading steps, which has been used again in the present study. The basic principle is that the elastic part of stress increments is calculated from the local strains and the remaining (inelastic) part of the stress increments is calculated from the nonlocal (spatially averaged) strains.

It should be noted that the present nonlocal cyclic microplane model yields nonsymmetric tangent stiffness matrix. Symmetrizing this matrix usually results in poor and uncertain convergence. Using constant stiffness method, one deals only with the elastic stiffness matrix, which is symmetric.

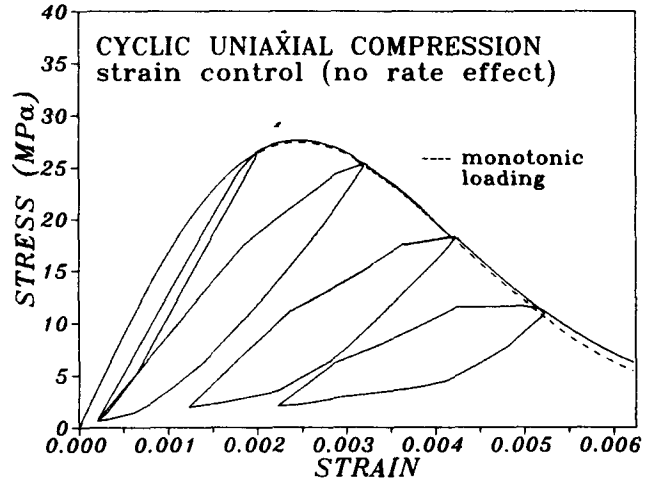

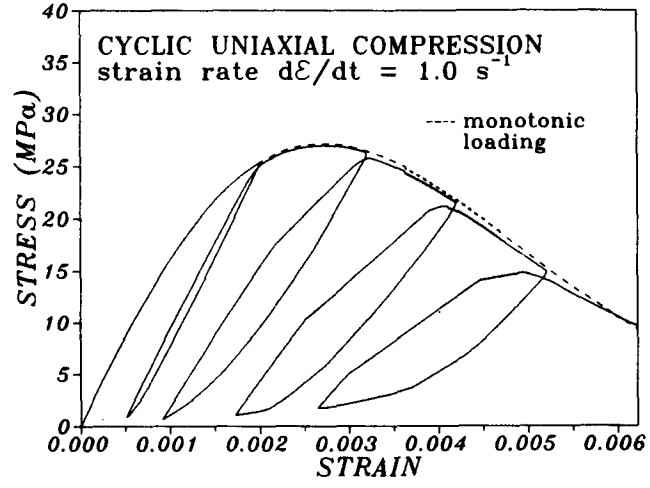

FIG. 5. Calculated Concrete Behavior in Uniaxial Cyclic Compression with Two Different Rates

The convergence then becomes reliable, but often rather slow. To improve the numerical effectiveness, the use of some nonsymmetric equation system solver might be useful.

Another point that calls for further study is the implementation of the distinction between local response (elastic stress increments) and nonlocal response (inelastic stress decrements). Due to the fact that the relative proportion of these two components changes, after many cycles it may happen that the middle flat portion of a pinched loop in shear loading

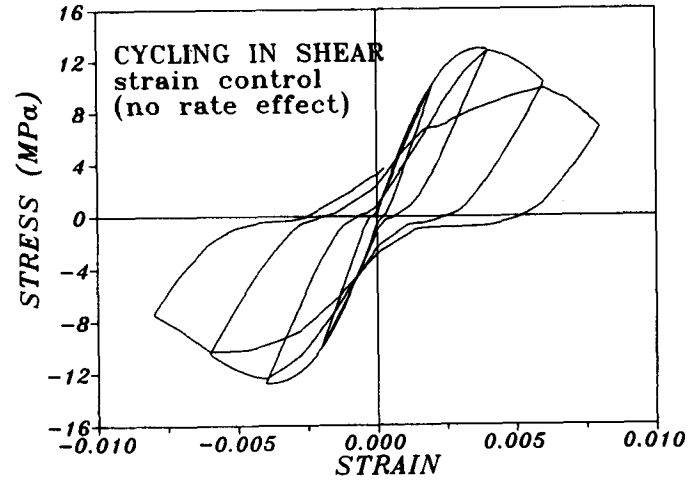

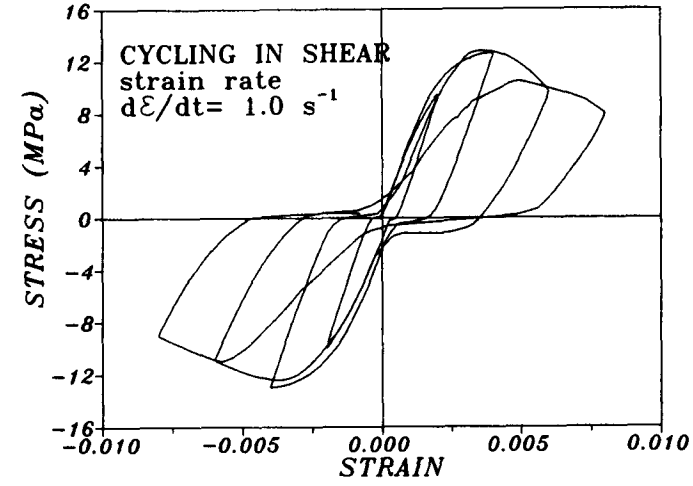

FIG. 6. Calculated Concrete Behavior in Cyclic Shear with Two Different Rates

becomes displaced vertically from the strain axis, which is nonrealistic. Some refined rule would have to be introduced to prevent this.

Numerical Examples

To demonstrate the capability of the present cyclic microplane model in predicting the cyclic behavior of concrete including the rate effect, numerical simulations for different stress-strain histories and different rates are carried out. The behavior of the model is first demonstrated on the material level, using only one uniformly strained finite element, loaded in three different ways as shown in Fig. 1(*d*). Cyclic behavior of the three-point-bend and compression specimens in plane stress is also simulated. It should be noted

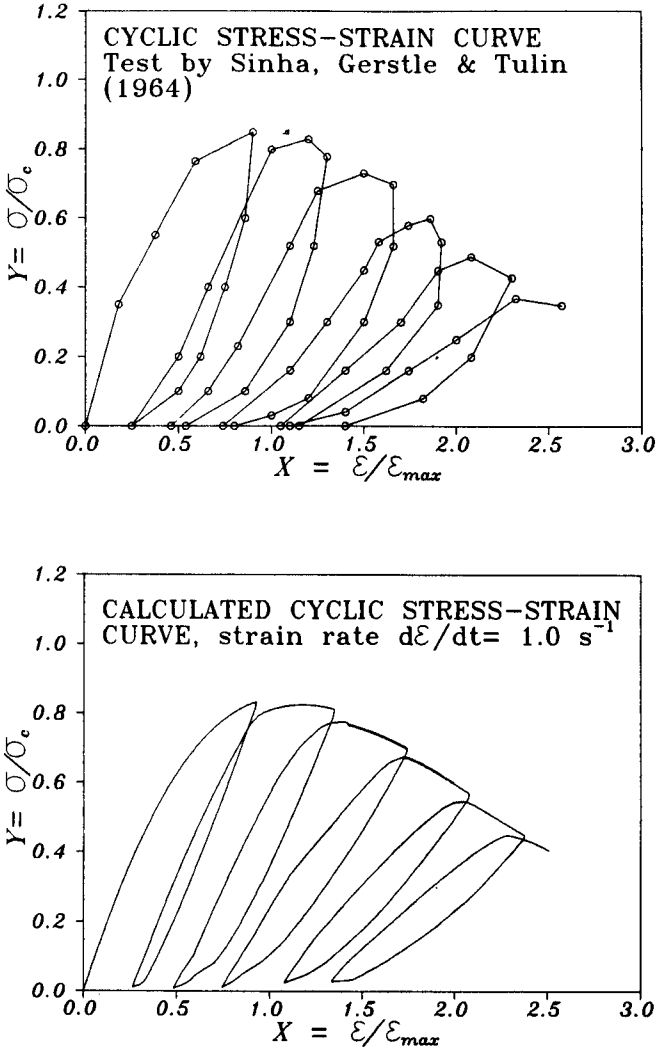

FIG. 7. Comparison between Test Data and Calculated Results for Cyclic Uniaxial Compression

that the plane stress state is a relatively more difficult state to simulate with the microplane model; the microplane model is a fully three-dimensional model and for the case of plane-stress finite elements the lateral strains (out-of-plane strains) need to be calculated from the condition that the lateral stresses are zero.

The basic material parameters used are: initial Young's modulus E^0 = 20,000 MPa, Poisson's ratio ν = 0.18, and relaxation time ρ = 0.01 sec. The microplane material parameters are chosen as follows: a = 0.005, b = 0.043, p = 0.75, q = 2.00, e_1 = 0.00007, e_2 = 0.0020, e_3 = 0.0020, e_4 = 0., m = 0.85, n = 2.25, and k = 2.25. These values are the same as in Bažant and Prat (1988), except m, n, and k (which have been adjusted such

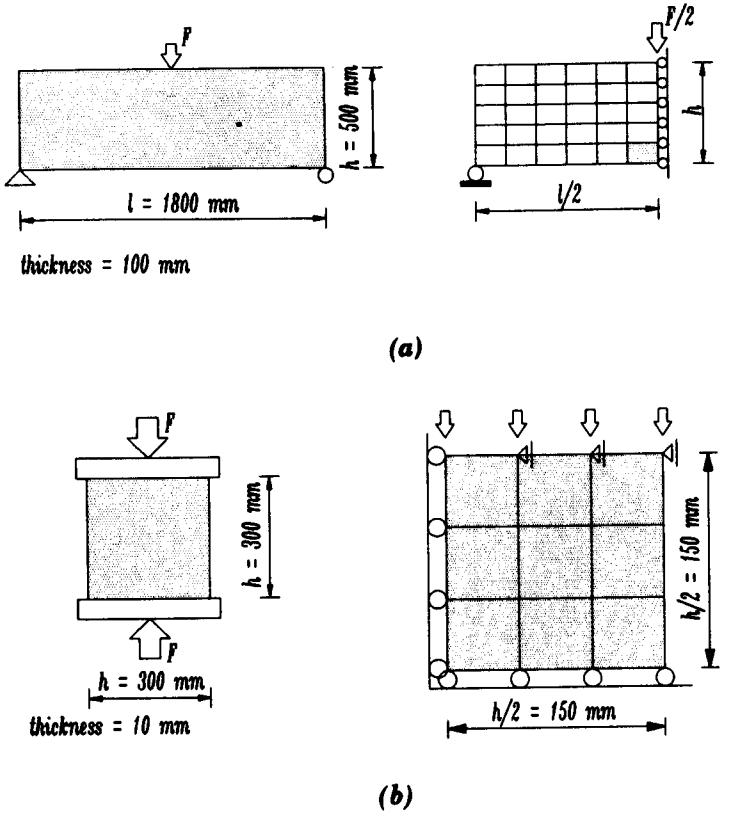

FIG. 8. Geometry and Finite Element Mesh for (a) Three-Point-Bend Specimen; (b) Compression Specimen

that the descending stress-strain curves would become steeper and would match the test results). The load was introduced by prescribing the displacement increases corresponding to different chosen strain rates in the finite element; $\dot{\varepsilon} \to \infty$, $\dot{\varepsilon}$ = 0.05 s^{-1}, and $\dot{\varepsilon}$ = 0.025 s^{-1}.

Fig. 3 shows the stress-strain curves obtained for the cases of uniaxial monotonic tension and compression, with different prescribed strain rates. Similar calculations, using again different strain rates, are carried out for the case of cyclic tension (Fig. 4), cyclic compression (Fig. 5), and cyclic shear (Fig. 6). Fig. 7 shows the comparison between the uniaxial cyclic test results of Sinha et al. (1964) and the present calculations.

The present results roughly agree with the general picture known from tests. This indicates that the present cyclic microplane model may be expected to realistically describe the cyclic behavior of concrete in diverse situations (van Mier 1984; Reinhardt and Cornelissen 1984), using the same material parameters for all situations.

Furthermore, the results indicate that the strain rate has a significant influence on the shape of the stress-strain curves. If the rate of loading decreases, the peak stress also decreases while the postpeak descending stress-strain curve becomes less steep. The present model can predict the

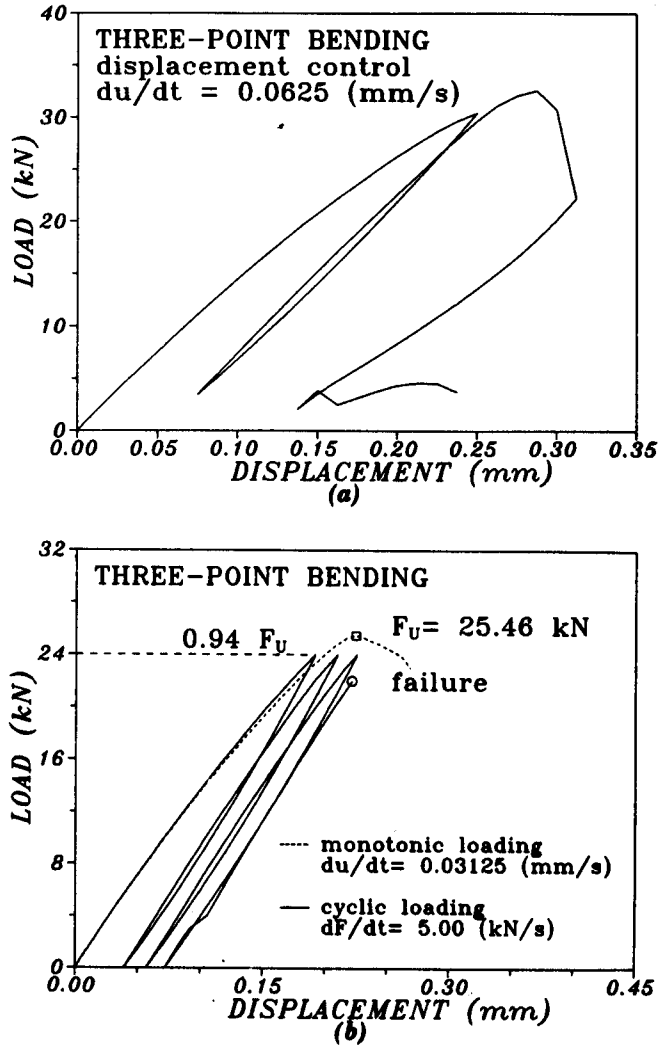

FIG. 9. Load-Displacement Curve of Three-Point Bend Specimen with Cycling: (a) in Postpeak Strain-Softening Range; (b) before Reaching Peak Load

drop of stresses after repeated unloading-reloading cycles in postpeak strain softening. As will be demonstrated later, this effect is significant when simulating the structural behavior.

To demonstrate finite element applications, the behavior of unnotched bending [Fig. 8(a)] and compression [Fig. 8(b)] specimens is analyzed. Four-node isoparametric quadrilateral plane-stress finite elements with four integration points are used. In both cases, symmetric response is assumed (Fig. 8). The material parameters are the same as in the previous examples, except that $e_1 = 0.00004$ and $m = 0.5$ in the case of the notched three-point bend specimen (due to reduced tensile strength).

Fig. 9(a) shows the load-displacement curve obtained for the bending

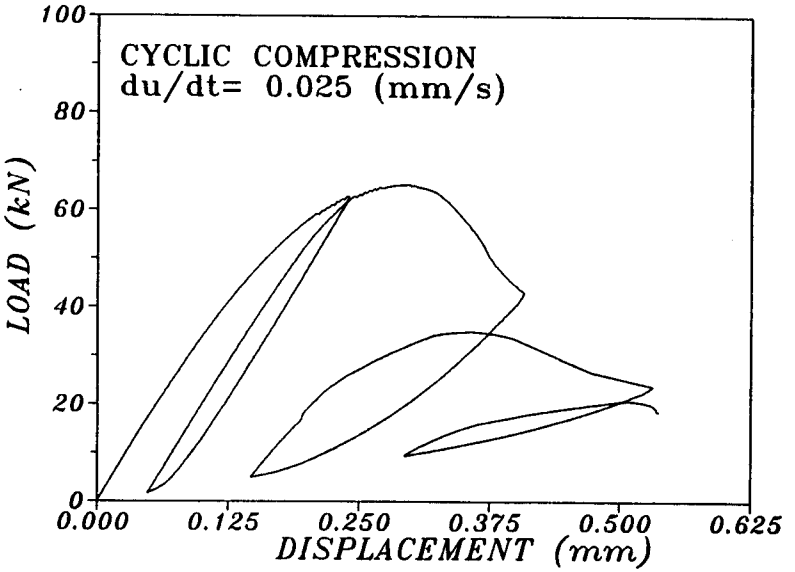

FIG. 10. Load-Displacement Curve for Specimen with Fixed Loading Platens Loaded in Cyclic Compression

specimen. The specimen is loaded prescribing displacement increments at the loaded node (see Fig. 8). The displacement rate is $\dot{u} = 0.0625$ mm s^{-1}. One cycle is performed prior to the peak load, and the next cycle late in the softening range. After the second cycle strength decreases, i.e., the material becomes damaged, and after repeated loading a significant decrease of strength is observed.

In the subsequent calculations of the same specimen, one finite element at the bottom of the specimen is assumed to be weaker, having a tensile strength limit 10% lower than the other elements (the shaded element in Fig. 8). The specimen is loaded repeatedly up to 94% of the peak load obtained for monotonic loading. This is followed by cyclic loading between 0 and 94% of this peak load. The loading consists of prescribing force F at the specimen top with the rate of increase $dF/dt = 5.0$ kNs^{-1}. The results indicate [Fig. 9(b)] a significant increase of the displacements due to material damage. Material damage due to cycling causes failure to occur already after the third cycle, just before reaching the monotonic descending branch [see Fig. 9(b)].

Fig. 10 shows the load-displacement cyclic response of a cubic compression specimen, subjected to controlled displacement u at the top of the specimen increasing at the rate $\dot{u} = 0.025$ mm s^{-1}. To simulate bonded (nonsliding) rigid platens at the top and bottom of the specimen, the horizontal displacements of the top nodes in the finite element mesh are fixed as zero. The calculated load-displacement curve indicates large residual stresses and strains, and a significant decrease of the concrete strength after reloading. These effects are stronger than those obtained by using only one finite element.

Generally, the calculated hysteretic loops in the preceding figures are wider when the rate effect is taken into account, and have approximately the correct area (as observed in tests of this type). In agreement with lab-

oratory observations, the unloading diagram begins with a steep slope that can even be steeper than the initial elastic slope (this is due to stress relaxation). For shear cycling, the calculated hysteretic loops exhibit the characteristic pinched form with an almost zero slope near the crossing of the strain axis, also known from experiments.

The aim of the present examples was to demonstrate that the present model is able to qualitatively predict the behavior of concrete at different rates of loading and for different stress-strain situations. Further work is needed in order to quantitatively verify the model by fitting a number of tests known from the literature.

Conclusions

1. The present, fully three-dimensional cyclic microplane model appears capable of realistically describing the behavior of plain concrete under a broad range of strain states and histories using the same material parameters. Together with the nonlocal strain concept, the model may be expected to provide effective finite element description of the failure process in concrete structures under rather general loading types and histories.
2. The rate effect can be implemented in the microplane model by combining damage with the Maxwell rheologic model. The model is able to give an approximately correct hysteretic loop area and a steep initial unloading slope. For shear, it exhibits the pinched form of hysteretic loops. Generally, increasing the rate increases the concrete strength and the postpeak descending branch of the stress-strain curve becomes steeper.
3. The examples indicate that the cyclic microplane model, together with rate effect, predicts material damage due to repeated unloading-reloading cycles quite realistically.

Acknowledgments

Partial financial support for nonlocal analysis was received from APOSR (under Grant 91-0140 to Northwestern University), and for the underlying fracture studies from the Center for Advanced Cement-Based Materials at Northwestern University and Institut für Werkstoffe im Bauwesen, Universität Stuttgart. Most of the paper was written during the second writer's sojourn at Lehrstuhl A für Mechanik, Technische Universität München, supported under A. von Humboldt Award of Senior U.S. Scientist. Thanks are due to Visiting Scholar T. Hasegawa for some thought-provoking comments.

Appendix. References

Batdorf, S. B., and Budianski, B. (1949). "A mathematical theory of plasticity based on the concept of slip." *Technical Note No. 1971*, National Advisory Committee for Aeronautics, Washington, D.C.
Bažant, Z. P. (1971). "Numerically stable algorithm with increasing time steps for integral-type aging creep." *Proc. First International Conference on Structural Mechanics in Reactor Technology*, T. A. Jaeger, ed., Berlin, Vol. 4, 119–126.
Bažant, Z. P. (1976). "Instability, ductility, and size effect in strain-softening concrete." *J. Engrg. Mech.*, ASCE, 102(2), 331–334.
Bažant, Z. P. (1984). "Microplane model for strain-controlled inelastic behavior." *Mechanics of engineering materials*, C. S. Desai and R. H. Gallager, eds., John Wiley and Sons, New York, N.Y., 45–59.
Bažant, Z. P., and Chern, J.-C. (1985). "Strain softening with creep and exponential algorithm." *J. Engrg. Mech.*, ASCE, 111(3), 391–415.
Bažant, Z. P., and Lin, F.-B. (1988). "Non-local yield limit degradation." *Int. J. Numer. Methods Engrg.*, 26, 1805–1823.
Bažant, Z. P., and Oh, B.-H. (1985). "Microplane model for progressive fracture of concrete and rock." *J. Engrg. Mech.*, ASCE, 111(4), 559–582.
Bažant, Z., and Ožbolt, J. (1990a). "Microplane model for cyclic triaxial behavior of concrete." Structural Engineering Report, Dept. of Civ. Engrg., Northwestern Univ., Evanston, Ill.
Bažant, Z. P., and Ožbolt, J. (1990b). "Nonlocal microplane model for fracture, damage, and size effect in structures." *J. Engrg. Mech.*, ASCE, 116(11), 2485–2504.
Bažant, Z. P., and Pijaudier-Cabot, G. (1987). "Modeling of distributed damage by nonlocal continuum with local strain." *Preprints, Fourth Int. Conf. on Numerical Methods in Fracture Mech., San Antonio, Texas, March*, A. R. Luxmore et al., eds., Pineridge Press, Swansea, United Kingdom, 411–432.
Bažant, Z. P., and Pijaudier-Cabot, G. (1988). "Nonlocal continuum damage, localization instability and convergence." *J. Appl. Mech. Trans. ASME*, 55, 287–293.
Bažant, Z. P., and Prat, P. C. (1988). "Microplane model for brittle-plastic material—parts I and II." *J. Engrg. Mech.*, ASCE, 114(10), 1672–1702.
Bažant, Z. P., and Wu, S. T. (1974). "Rate type creep law of aging concrete based on Maxwell chain." *Materials and Structures, (RILEM, Paris)*, 7(37), 45–60.
Eringen, A. C. (1965). "Theory of micropolar continuum." *Proc. 9th Midwestern Mech. Conf.*, University of Wisconsin-Madison, 23–40.
Eringen, A. C. (1966). "A unified theory of thermomechanical materials." *Int. J. Eng. Sci.*, 4, 179–202.
Eringen, A. C., and Edelen, D. G. D. (1972). "On nonlocal elasticity." *Int. J. Eng. Sci.*, 10, 233–248.
Hasegawa, T., and Bažant, Z. P. (1991). "Nonlocal microplane model with rate effect for concrete." *Struct. Engrg. Report 91-9/919*, Dept. of Civ. Engrg., Northwestern Univ., Evanston, Ill.
Kröner, E. (1968). "Interrelations between various branches of continuum mechanics." *Mechanics of Generalized Continuua*, E. Kröner, ed., Springer, Berlin, Germany, 330–340.
Krumhansl, J. A. (1968). "Some considerations of the relations between solid state physics and generalised continuum mechanics." *Mechanics of Generalized Continuum*, E. Kröner, ed., Springer, Berlin, Germany, 298–331.
Pijaudier-Cabot, G., and Bažant, Z. P. (1987). "Nonlocal damage theory." *J. Engrg. Mech.*, ASCE, 113, 1512–1533.
Reinhardt, H. W., and Cornelissen, H. A. W. (1984). "Post-peak cyclic behavior of concrete in uniaxial tensile and alternating tensile and compressive loading." *Cem. Concr. Res.*, 14, 263–278.
Sinha, B. P., Gerstle, K. H., and Tulin, L. G. (1964). "Stress-strain relations for concrete under cyclic loading." *J. Amer. Concrete Inst.*, 61(2) 195–211.
Taylor, G. I. (1938). "Plastic strain in metals." *J. Inst. of Metals*, 62, 307–324.
Zienkiewicz, O. C., and Pande, G. N. (1977). "Time-dependent multi-laminate model of rocks—a numerical study of deformation and failure of rock masses." *Int. J. Numerical and Analytical Methods in Geomechanics*, 1, 219–247.